Copyright WILEY-VCH Verlag GmbH & Co. KGaA, 69469 Weinheim, Germany, 2018.

Supporting Information

Exciton and Charge Carrier Dynamics in Highly Crystalline PTQ10:IDIC Organic Solar Cells.

Hyojung Cha, Yizhen Zheng, Yifan Dong, Hyun Hwi Lee, Jiaying Wu, Helen Bristow, Jiangbin Zhang, Harrison Ka Hin Lee, Wing C. Tsoi, Artem A. Bakulin, Iain McCulloch, James R. Durrant

Full name.

Experimental.

Calculation of Förster Distance.

Table S1. *J-V* characteristics of PTQ10:IDIC blend solar cells with various composition ratios.

Figure S1. (a) Absorption coefficient for neat PTQ10, neat IDIC and PTQ10:IDIC blend films with various composition ratios. (b) Normalised UV-Visible absorption spectra and steady state PL spectra of neat PTQ10 and IDIC films.

Figure S2. (a) Normalised photoluminescence (PL) and (b) normalised electroluminescence (EL) spectra of PTQ10:IDIC blend devices with different ratios.

Figure S3. EQE spectra of the inverted structured OSCs based on PTQ10:IDIC blends with different composition ratios.

Table S2. PL quenching (PLQ) yield of PTQ10:IDIC blend films. All blends were excited at 450 nm. PL quenching yield of donor (acceptor) was calculated with PL intensity difference in blends measured at 660 nm (760 nm).

Table S3. π-π distances and calculated domain sizes in neat PTQ10, neat IDIC and PTQ10:IDIC blends.

Figure S4. (a) PL kinetics for PTQ10 (donor) film and blend films with different composition ratios measured by TCSPC, excited at 467 nm and probed at 660 nm. (b) PL kinetics for acceptor IDIC film and blend films with different composition ratios measured by TCSPC. Black curve: instrument response function (IRF), excited at 635 nm and probed at 760 nm.

Table S4. Calculated exciton diffusion length of PTQ10 and IDIC at various energy density. n_0: exciton density, $t_{1/2}$: half-lifetime of exciton probed at 1005nm. k: exciton intrinsic decay rate constant, γ: EEA rate coefficient, α: modify factor, D: diffusion coefficient and L_d: diffusion length.

Figure S5. Transient absorption spectra for (a) neat IDIC and (b) PTQ10:IDIC blend (1:1.5) film, excited on IDIC at 700 nm with energy density of 12.5 μJ cm^{-2}. Transient absorption spectral components and relevant kinetics extracted from transient absorption spectra with excitation at 700 nm for neat IDIC and PTQ10:IDIC blend films with energy density of (c) 12.5 μJ cm^{-2} and (d) 12.5 μJ cm^{-2}

Figure S6. (a) Transient absorption spectra for PTQ10:IDIC blend film of 1:1.5 ratio, excited on IDIC at 700 nm with energy density of 2.5 μJ cm^{-2} and (b) deconvoluted spectra for PTQ10:IDIC blend.

Figure S7. Energy dependent transient absorption decay dynamics for PTQ10:IDIC (1:1.5) blend film probed at (a) charge transfer (CT) states and (b) charge separated (CS) states.

Figure S8. Energy density dependent dynamics for PTQ10:IDIC (1:1.5) blendfilm probed at CS states (P2) including average exciton separations at the initial exciton densities between 5.5×10^{17} and 1×10^{19} cm^{-3} (2.5 – 25 μJ cm^{-2}) after global analysis.

Figure S9. Transient absorption spectra for PTQ10:IDIC blend film of (a) 1:0.5, (b) 1:1.5, and (c) 1:5 ratio, excited on IDIC at 700 nm with energy density of 2.5 μJ cm^{-2}. Transient absorption spectral components and relevant kinetics extracted from transient absorption spectra with excitation at 700 nm for PTQ10:IDIC blend films of (d) 1:0.5, (e) 1:1.5, (f) 1:5 ratios, respectively, using the global analysis.

Figure S10. Analysis of charge transport and bimolecular recombination in PTQ10:IDIC device. (a) Dependence on open circuit voltage and (b) the corresponding charge carrier lifetimes measured by TPV decays, as a function of charge densities.

Full name:

PTQ10: poly[(thiophene)-alt-(6,7-difluoro-2-(2-hexyldecyloxy)quinoxaline)]

IDIC: 2,7-bis(2-methylene-(3-(1,1-dicyanomethylene)-indanone))- 4,4,9,9-tetrahexyl-s-indaceno[1,2-b:5,6-b']dithiophene

Experimental.

Organic Photovoltaic Devices. Organic solar cells were fabricated with an inverted architecture (glass/ITO/ZnO/PTQ10:IDIC/MoO_3/Ag). Glass substrates were used with pre-patterned indium tin oxide (ITO). These were cleaned by sonication in detergent, deionized water, acetone and isopropanol, followed by oxygen plasma treatment. ZnO layers were deposited by spin-coating a zinc acetate dihydrate precursor solution (60.4 µl 1-ethanolamine in 2 ml 2-methoxyethanol) followed by annealing at 150 °C for 10 min, giving layers of 30 nm. The PTQ10:IDIC active layers with different donor:acceptor ratio were deposited from 25 mg/ml solutions in chloroform by dynamic spin-coating at 2,000-3,000 r.p.m. After spin-coating, the active layers were annealed at 140 °C for 5 min for the devices with TA treatment in glove box. MoO_3 (10 nm) and Ag (100 nm) layers were deposited by evaporation through a shadow mask yielding active areas of 0.045 cm^2 in each device. Current-Voltage (*J–V*) characteristics of optimised devices were measured with a Keithley 2400 source meter ranging from -1.2 V to 1.2 V and corrected for spectral mismatch. Measurement was carried out under an AM 1.5 G solar illumination of 100 mW cm^{-2} using a filtered 300W xenon lamp (Oriel Instruments). A calibrated silicon photodiode was used as a reference for the *J–V* measurements. The devices were sealed in a chamber with a quartz window on the top for illumination. The chamber was filled with N_2 to protect the devices. In EQE measurements, a 100W tungsten halogen lamp (Bentham IL1 and Bentham 605 stabilized current power supply) was used as photon source. Incident light passed through a monochromator with a computer-controlled step motor, and a UV-enhanced silicon photodiode was used to calibrate its photon flux. A 590 nm long-pass filter was used to block light from second-order diffraction. Measurement duration for a given wavelength was sufficient to ensure the current is stable.

UV-Visible Absorption and Photoluminescence (PL) Spectroscopies. UV-Visible spectra of the thin films were acquired with a PerkinElmer Lambda 25 spectrometer in air. The PL spectra were measured with a Fluorolog-3 spectrofluorometer (Horiba Jobin Yvon). All film samples

were spin cast on glass substrates.

Time-correlated single-photon counting (TCSPC). The TCSPC curves were measured with a Deltaflex PPD900 equipped with 467 nm and 665 nm picosecond laser diodes to selectively excite donor PTQ10 and acceptor IDIC respectively with a 1.0 MHz repetition rate. The detection wavelength was set at the PL peak of the material. The detection rate was limited lower than 60000 to avoid detector saturation and collection bias.

Electroluminescence (EL). The EL measurements were performed using a Renishaw inVia Raman system and a source measurement unit (Keithley 236). 50x objective with a numerical aperture of 0.5 was used to focus on the device area. Voltage between 6 V and 20 V was applied to the device during the measurement and the acquisition time was 30s for each spectrum.

Grazing Incidence Wide Angle X-ray Scattering (GIWAXS) Characterisation. GIWAXS measurements were performed at beamline 5A at the Pohang Accelerator Laboratory (PAL) in South Korea. Samples were prepared on ITO/ZnO substrates using identical blend solutions as those used in devices. The 10 keV X-ray beam was incident at a grazing angle of 0.12°–0.16°, selected to maximise the scattering intensity from the samples. The scattered X-rays were detected using a Dectris Pilatus 2M photon counting detector.

Femtosecond Transient Absorption Spectroscopy (fs-TAS). Laser pulses with wavelength of 800 nm, and time duration of 90 fs were generated from a Ti:Sapphire laser system (Newport Corporation). They were split into two parts for generating pump and probe pulses respectively. The pump pulses were generated from a TOPAS-Prime optical parametric amplifier (Light Conversion). The pump pulse was focused on the sample with the spot area of about 0.2 mm^2. The intensity of pump pulse was controlled by a variable neutral-density filter wheel. The pump pulse was chopped by a synchronized chopper. A near-infrared continuum probe (900 nm – 1450 nm) was generated in a sapphire crystal. The probe light was collimated and focused with a parabolic reflector onto the sample. A HELIOS transient absorption spectrometer (Ultrafast system) was used to measure the transient absorption spectra with specific time delays. The

time delay between pump and probe light was controlled by a delay line. The sample films were mounted in a quartz sample holder for all measurements.

Global Analysis (GA). The raw results from TAS are always complicated because of the overlap of various species in the blends. In order to decompose the dynamics of these species, Genetic algorithm was used as a global fitting method. Basically, a mass of spectra sets was generated randomly to fit the raw data, and results were evaluated by the sum of the absolute value of residuals. The best fitted spectra set was then modified by mutating with each other to avoid local minima. Additional penalty was added for nonphysical results, so the method will avoid pure mathematical solutions in a large part.

Calculation of Förster distance. Förster distance[1], R_0, at which the energy transfer efficiency is 50%, is estimated using the following equation,

$$R_0 = 0.21(J(\lambda)\, q_d\, n^{-4}\, \kappa^2)^{1/6} \text{ where, } J(\lambda) = \int F_D(\lambda)\, \varepsilon_A(\lambda)\, \lambda^4\, d\lambda \;/\; \int F_D(\lambda) d\lambda$$

κ is the orientation factor between the donor and acceptor dipoles,

q_d is the average donor fluorescence quantum yield in the absence of the acceptor,

n is the medium refractive index,

$J(\lambda)$ represents the overlap integral, characterized by normalized spectrum overlap between donor molecule's $F_D(\lambda)$, fluorescence intensity in arbitrary unit,

$\varepsilon_A(\lambda)$, acceptor's absorption coefficient in cm^{-1} scaled by λ, wavelength (in nm) to the fourth power.

$\kappa^2 = 2/3$ for random orientation of dipoles; $n = 1.45$ (for most organic systems); $q_d = 0.1$; $J(\lambda) = 2.4 * 10^{16}\ cm^{-1}\ nm^4$ at 700 nm.

Substituting the above values in the equation, we found the Förster distance, R_0 to be **5.9 nm**, which is a longer Förster radius compared to other blend system due to entirely overlapped donor emission and acceptor absorption and high absorption coefficient.

[1] A. A. Mohapatra, V. Kim, B. Puttaraju, A. Sadhanala, X. Jiao, C. R. McNeill, R. H. Friend, S. Patil, *ACS Appl. Energy Mater.* **2018**, *1*, 4874.

Table S1. *J-V* characteristics of PTQ10:IDIC blend solar cells with various composition ratios.

	J_{SC} (mA cm^{-2})	V_{OC} (V)	FF	PCE_{ave} (%)
1:0.5	9.8 (± 0.6)	0.99 (± 0.01)	0.37 (± 0.03)	3.2 (± 0.5)
1:1.5	20.2 (± 0.3)	0.97 (± 0.01)	0.63 (± 0.02)	12.4 (± 0.2)
1:3	19.3 (± 0.3)	0.94 (± 0.01)	0.61 (± 0.02)	11.1 (± 0.2)
1:5	15.9 (± 0.4)	0.90 (± 0.01)	0.57 (± 0.02)	8.2 (± 0.25)

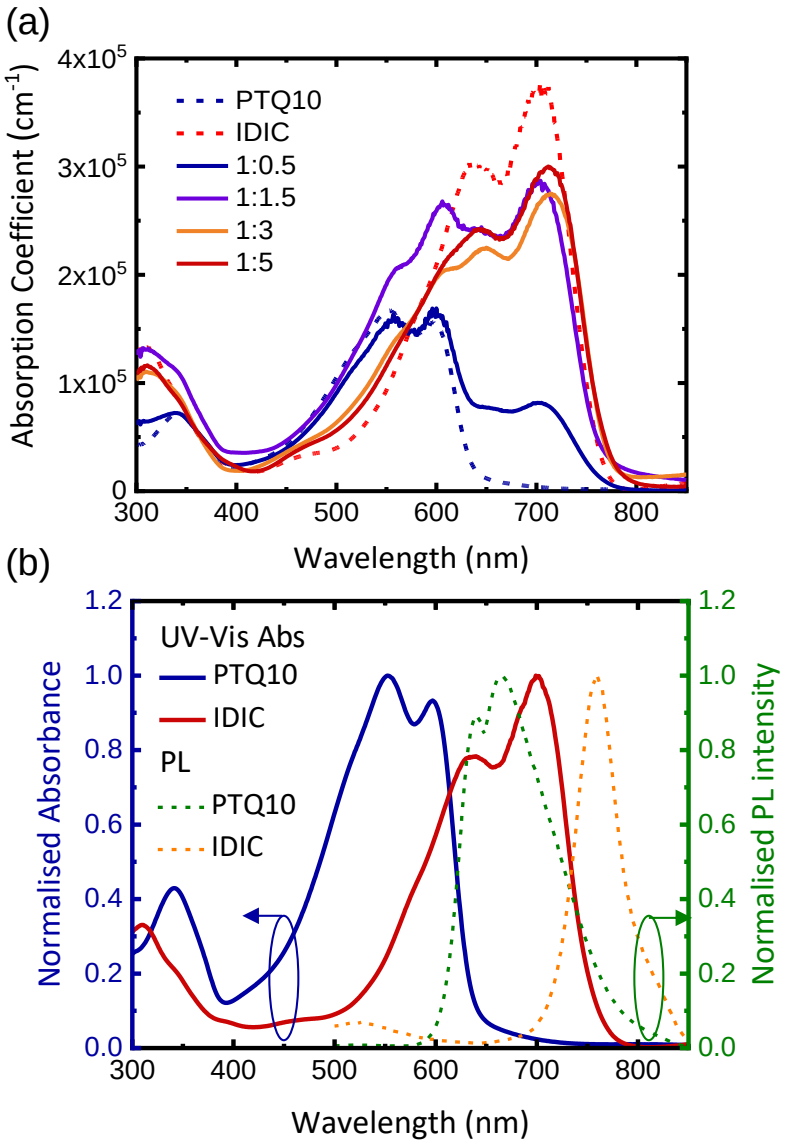

Figure S1. (a) Absorption coefficient for neat PTQ10, neat IDIC and PTQ10:IDIC blend films with various composition ratios. (b) Normalised UV-Visible absorption spectra and steady state PL spectra of neat PTQ10 and IDIC films.

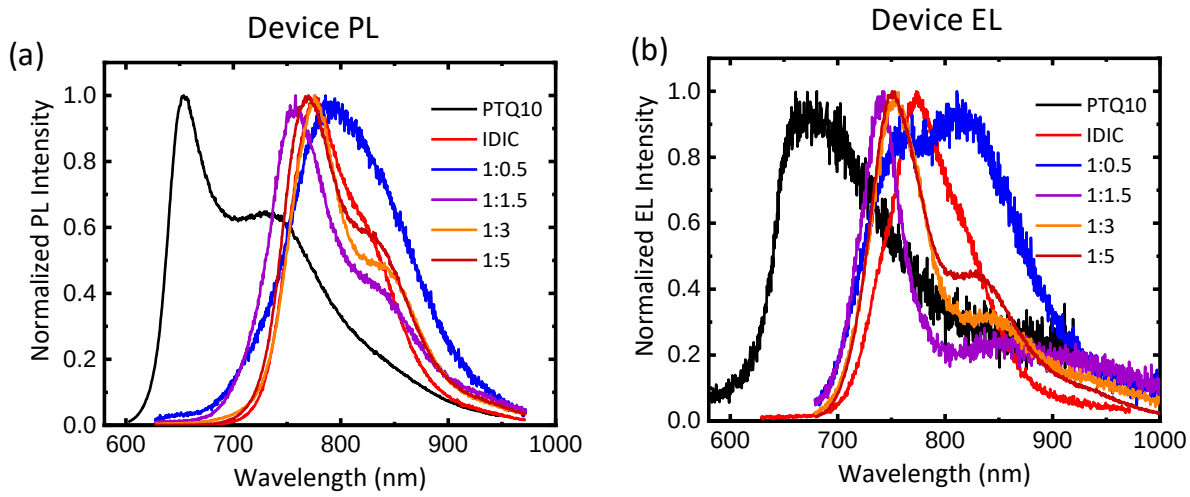

Figure S2. (a) Normalised photoluminescence (PL) and (b) normalised electroluminescence (EL) spectra of PTQ10:IDIC blend devices with different ratios.

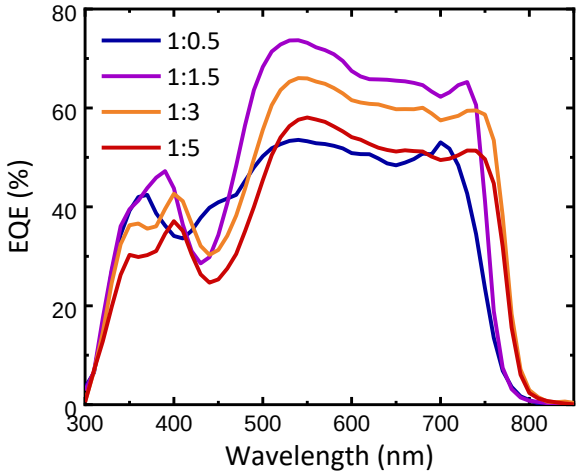

Figure S3. EQE spectra of the inverted structured OSCs based on PTQ10:IDIC blends with different composition ratios.

Table S2. PL quenching (PLQ) yield of PTQ10:IDIC blend films. All blends were excited at 450 nm. PL quenching yield of donor (acceptor) was calculated with PL intensity difference in blends measured at 660 nm (760 nm).

	1:0.5	1:1.5	1:3	1:5
PLQ_D (%)	99.43	99.66	99.28	99.57
PLQ_A (%)	97.46	97.15	86.70	83.91

Table S3. π-π distances and calculated domain sizes in neat PTQ10, neat IDIC and PTQ10:IDIC blends.

Plane	Materials	Q vector	FWHM	2 theta	π-π distance (Å)	Domain size (nm)
OOP (010)	PTQ10	18	0.75	2.87	3.49	8.53
OOP (010)	IDIC	18.21	0.89	2.93	3.45	7.19
OOP (010)	1:0.5	18.06	1.29	2.89	3.48	4.96
OOP (010)	1:1.5	18.18	0.78	2.92	3.45	8.20
OOP (010)	1:3	18.2	0.7	2.93	3.45	9.14
OOP (010)	1:5	18.23	0.6	2.94	3.45	10.66

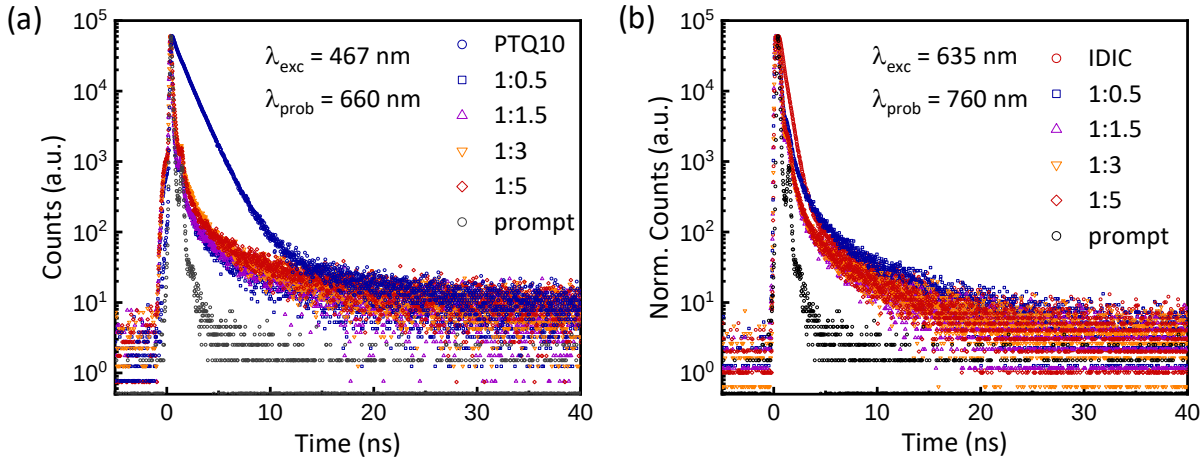

Figure S4. (a) PL kinetics for PTQ10 (donor) film and blend films with different composition ratios measured by TCSPC, excited at 467 nm and probed at 660 nm. (b) PL kinetics for acceptor IDIC film and blend films with different composition ratios measured by TCSPC. Black curve: instrument response function (IRF), excited at 635 nm and probed at 760 nm.

Table S4. Calculated exciton diffusion length of PTQ10 and IDIC at various energy density. n_0: exciton density, $t_{1/2}$: half-lifetime of exciton probed at 1005nm. k: exciton intrinsic decay rate constant, γ: EEA rate coefficient, α: modify factor, D: diffusion coefficient and L_d: diffusion length.

Donor PTQ10

Energy μJ cm^{-2}	n_0 (×10^{16})	$t_{1/2}$ ps	k	α	γ (×10^{-8}) cm^3 s^{-1}	D cm^2 s^{-1}	L_d nm
0.25	2.87	820	8.45×10^8				
2.5	28.7	208		0.25	1.24	0.00342	16.7
12.5	144	40		0.049	1.65	0.00457	19.4
25	287	20		0.024	1.70	0.00469	19.6
100	1150	5.5		0.0067	1.57	0.00435	18.9

Acceptor IDIC

Energy μJ cm^{-2}	n_0 (×10^{16})	$t_{1/2}$ ps	k	α	γ (×10^{-8}) cm^3 s^{-1}	D cm^2 s^{-1}	L_d nm
1	14	21	3.30×10^{10}				
2.5	35	8.3		0.40	2.05	0.0566	10.9
12.5	175	2.6		0.12	1.92	0.0529	10.5
25	350	1.64		0.078	1.60	0.0442	9.6
100	1400	0.8		0.038	0.86	0.0237	7.1

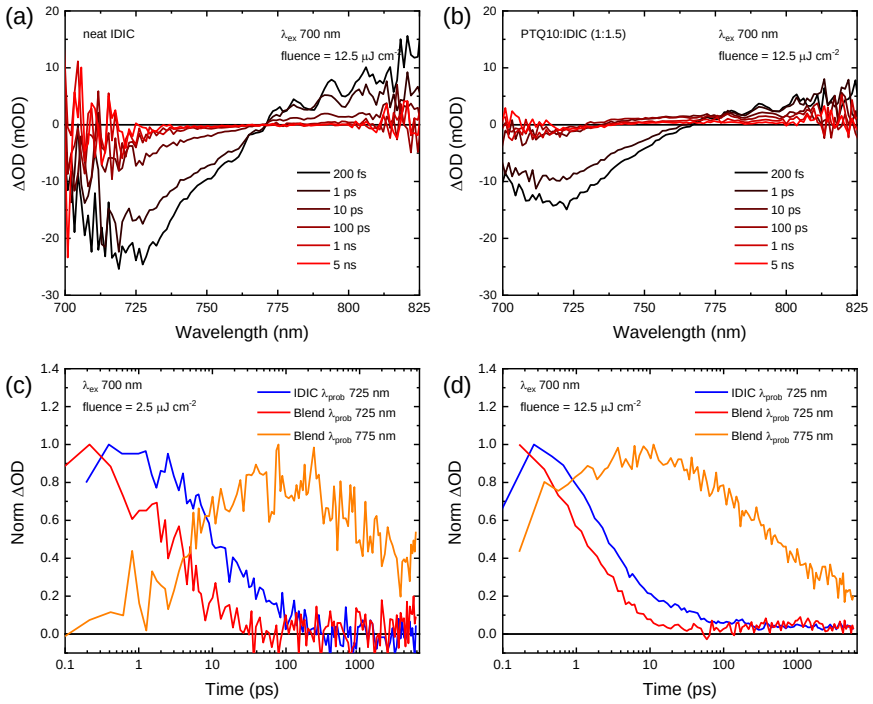

Figure S5. Transient absorption spectra for (a) neat IDIC and (b) PTQ10:IDIC blend (1:1.5) film, excited on IDIC at 700 nm with energy density of 12.5 μJ cm-2. Transient absorption spectral components and relevant kinetics extracted from transient absorption spectra with excitation at 700 nm for neat IDIC and PTQ10:IDIC blend films with energy density of (c) 2.5 μJ cm-2 and (d) 12.5 μJ cm-2

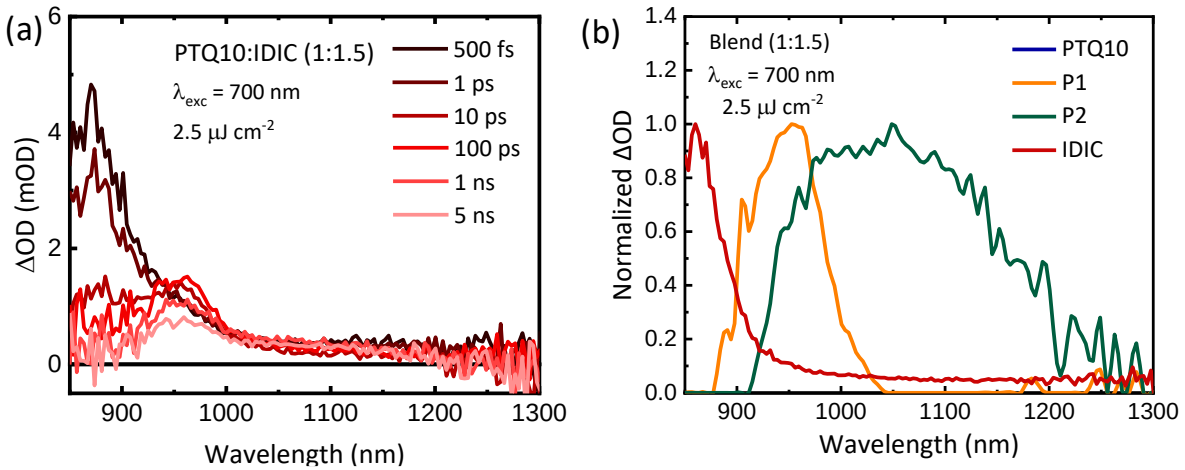

Figure S6. (a) Transient absorption spectra for PTQ10:IDIC blend film of 1:1.5 ratio, excited on IDIC at 700 nm with energy density of 2.5 μJ cm-2 and (b) deconvoluted spectra for PTQ10:IDIC blend.

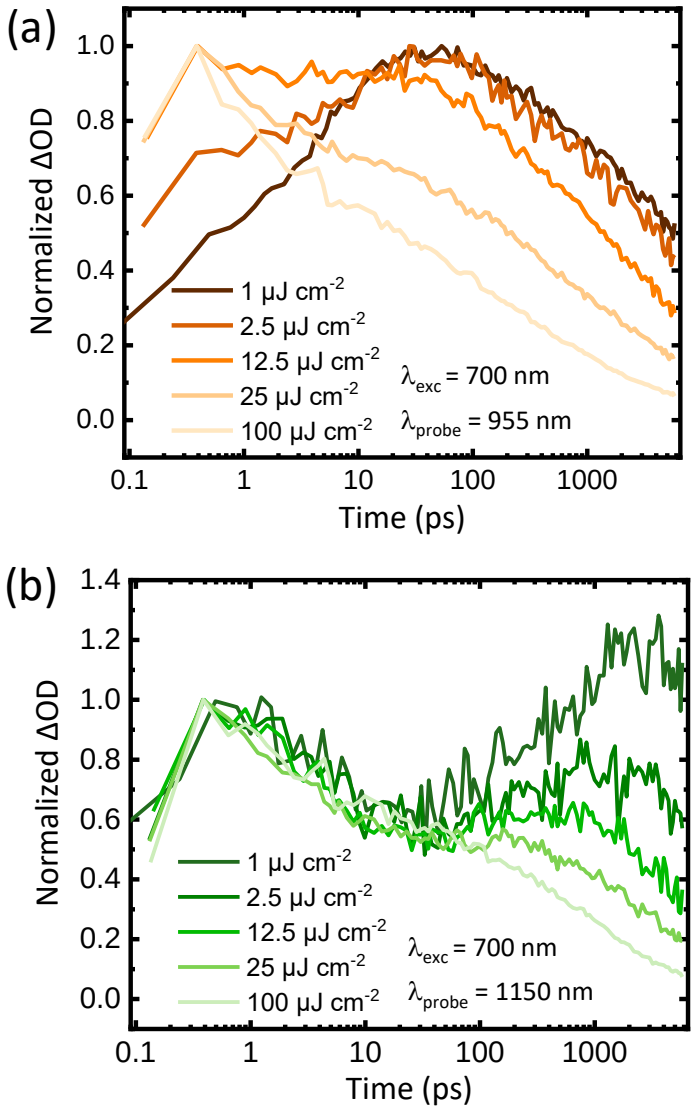

Figure S7. Energy dependent transient absorption decay dynamics for PTQ10:IDIC (1:1.5) blend film probed at (a) charge transfer (CT) states and (b) charge separated (CS) states.

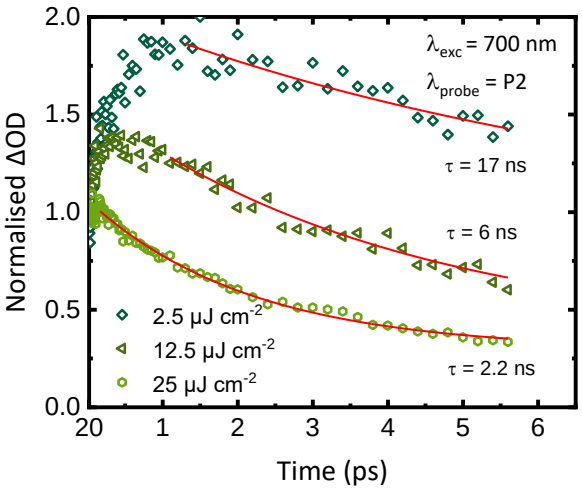

Figure S8. Energy density dependent dynamics for PTQ10:IDIC (1:1.5) blendfilm probed at CS states (P2) including average exciton separations at the initial exciton densities between 5.5×10^{17} and 1×10^{19} cm^{-3} (2.5 – 25 μJ cm^{-2}) after global analysis.

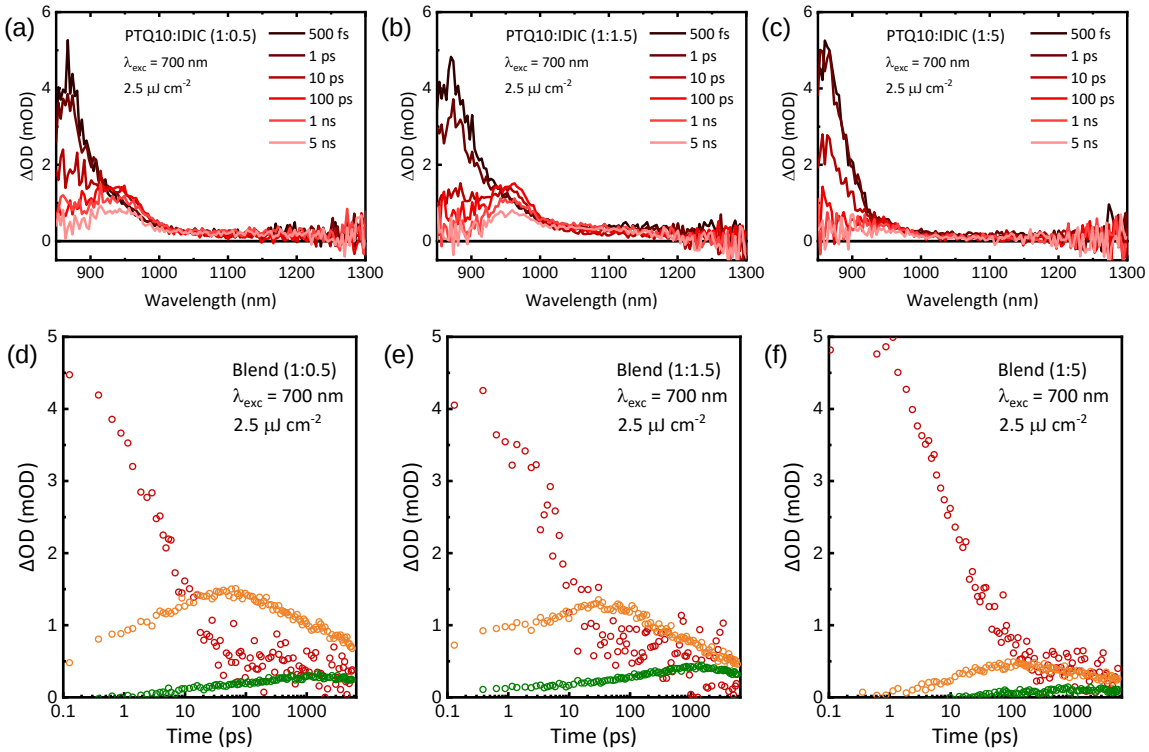

Figure S9. Transient absorption spectra for PTQ10:IDIC blend film of (a) 1:0.5, (b) 1:1.5, and (c) 1:5 ratio, excited on IDIC at 700 nm with energy density of 2.5 μJ cm-2. Transient absorption spectral components and relevant kinetics extracted from transient absorption spectra with excitation at 700 nm for PTQ10:IDIC blend films of (d) 1:0.5, (e) 1:1.5, (f) 1:5 ratios, respectively, using the global analysis.

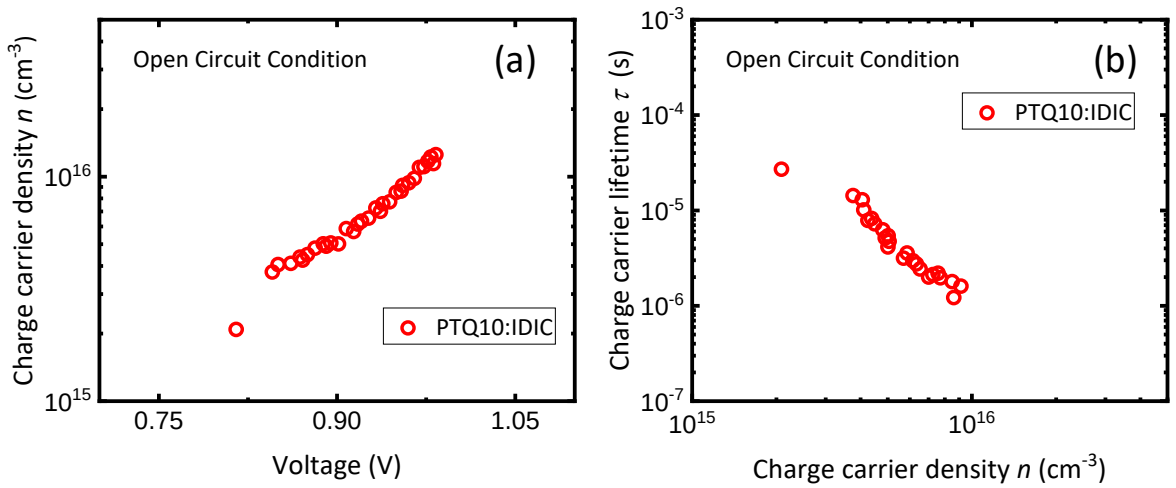

Figure S10. Analysis of charge transport and bimolecular recombination in PTQ10:IDIC device. (a) Dependence on open circuit voltage and (b) the corresponding charge carrier lifetimes measured by TPV decays, as a function of charge densities.